

Chapter 2

Experimental Stress Analysis of Unsymmetrical, Irregularly-Shaped Structure Containing an Arbitrarily-Shaped Hole

B. Kalayciogli, A. Alshaya, and R. Rowlands

Abstract This paper describes the ability to process load induced temperature information with an Airy stress function in real polar coordinates and some local known boundary conditions to determine the stresses experimentally in an isotropic linear elastic finite arbitrarily-shaped structure containing an irregularly-shaped hole. The proposed method simultaneously smooths the measured data, separates the stress components, and evaluates the individual stress components full-field, including at the boundary of the hole (location of highest tensile stress).

Keywords Thermoelastic stress analysis • Irregularly-shaped holes • Stress concertation • Airy stress function • Hybrid method

2.1 Introduction

References [1–3] treat non-circular cutouts using complex variables and conformal mapping but are restricted to infinitely large members having relatively simple and known external boundary conditions. References [4–16] combine thermoelastic stress data with a series solution of Airy stress function in either real or complex variables along with imposed traction-free boundary conditions on the edge of a hole to determine full-field individual components of stress, strain and displacements. Unlike with Fig. 2.1, all previous situations enjoyed a simple eternal shape, symmetry and/or necessitated imposing the boundary condition only on the internal boundary. Although a few cases imposed the internal boundary conditions discretely, most enabled imposing them analytically. The predominance of asymmetrically-loaded arbitrarily-shaped mechanical structures having irregularly-shaped holes necessitates the present technical extension.

Thermoelastic stress analysis (TSA) is a non-contacting, nondestructive experimental method for determining the full-field stresses in loaded members [17]. The technique enables the stress analysis of actual structures in their operating environment with a sensitivity comparable to that of strain gages. No surface preparation is required other than perhaps a flat black paint to provide an enhanced and uniform emissivity. For proportional loading under adiabatic, reversible elastic conditions, the stress- induce temperature information, S^* , is proportional to the changes in the sum of the normal stresses, S ,

$$S^* = K \Delta S = K \Delta (\sigma_1 + \sigma_2) = K \Delta (\sigma_{xx} + \sigma_{yy}) = K \Delta (\sigma_{rr} + \sigma_{\theta\theta}) = K \Delta (\sigma_{\xi\xi} + \sigma_{\eta\eta}) \quad (2.1)$$

where K is experimentally-determined thermoelastic material coefficient, and $\sigma_1, \sigma_2, \sigma_{rr}, \sigma_{\theta\theta}, \sigma_{xx}, \sigma_{yy}, \sigma_{\xi\xi}$, and $\sigma_{\eta\eta}$ are the normal stress components in the principal, polar, Cartesian rectangular coordinates, and normal and tangent to the edges of the structure, respectively. Combining experimental information with analytical and numerical tools enables one to separate stress components. The plate was sinusoidally compressed at 1334.46 ± 667.23 N at a rate of 20 Hz in a 20 kips capacity MTS hydraulic testing machine. The corresponding load-induced TSA data were recorded using a DeltaTherm model DT1410 system (Stress Photonics, Madison, WI) having a sensor array of 256 horizontal by 256 vertical pixels. The camera is cooled with liquid nitrogen to maintain the sensor at a very low temperature necessary for the accurate readings. The thermoelastic

B. Kalayciogli
Kirikkale University, Kirikkale, Turkey

A. Alshaya
Kuwait University, Kuwait, Kuwait

R. Rowlands (✉)
University of Wisconsin-Madison, Madison, WI, USA
e-mail: rowlands@engr.wisc.edu

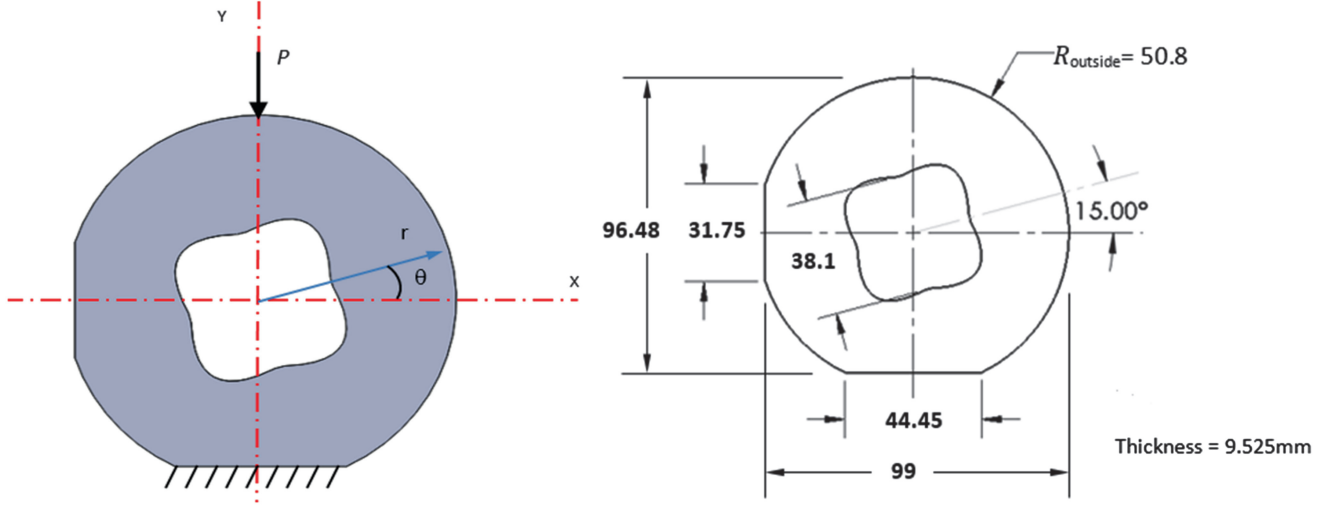


Fig. 2.1 CAD model of finite plate with arbitrary-shaped aluminum plate containing irregularly-shaped hole

signal, S^* , was recorded by the data acquisition system which is equipped with Delta Vision Software and TSA images were captured and averaged over two minute durations. Since TSA data typically are unreliable on and near an edge, no recorded TSA information was used within at least two pixel positions (0.92 mm) of the boundary.

2.2 Relevant Equations

For elasto-static plane isotropic problems in the absence of the body forces, the Airy stress function, Φ , satisfying stress equilibrium and strain compatibility conditions gives the biharmonic equation $\nabla^4 \Phi = 0$ where ∇^2 is the Laplacian operator and $\nabla^2 = \frac{\partial^2}{\partial r^2} + \frac{1}{r} \frac{\partial}{\partial r} + \frac{1}{r^2} \frac{\partial^2}{\partial \theta^2}$. The general solution to $\nabla^4 \Phi = 0$ in polar coordinates for the plate in Fig. 2.1 is [18]

$$\begin{aligned} \Phi = & a_0 + b_0 \ln r + c_0 r^2 + A_0 \theta + (a_1 r + \frac{c_1}{r} + d_1 r^3) \sin \theta + \left(a_1' r + \frac{c_1'}{r} + d_1' r^3 \right) \cos \theta \\ & + \sum_{n=2,3,\dots}^{\infty} (a_n r^n + b_n r^{n+2} + c_n r^{-n} + d_n r^{-(n-2)}) \sin n\theta \\ & + \sum_{n=2,3,\dots}^{\infty} (a_n' r^n + b_n' r^{n+2} + c_n' r^{-n} + d_n' r^{-(n-2)}) \cos n\theta \end{aligned} \quad (2.2)$$

where r is the radial coordinate measured from the center of the notch, θ is measured counter-clockwise from the horizontal x -axis as shown in Fig. 2.1, and N is the terminating index of the series which is any positive integer. The individual components of stresses in polar coordinate can be evaluated from

$$\sigma_{rr} = \frac{1}{r} \frac{\partial \Phi}{\partial r} + \frac{1}{r^2} \frac{\partial^2 \Phi}{\partial \theta^2}, \quad \sigma_{\theta\theta} = \frac{\partial^2 \Phi}{\partial r^2}, \quad \sigma_{r\theta} = -\frac{\partial}{\partial r} \left(\frac{1}{r} \frac{\partial \Phi}{\partial \theta} \right) \quad (2.3)$$

Determination of individual stresses, strains, or displacements necessitates evaluating the unknown Airy coefficients of Eq. 2.2. To help evaluate all of the Airy coefficients, boundary conditions in terms of stresses as shown in Fig. 2.2 were imposed discretely at multiple locations on the interior and exterior boundaries of the structure.

2.3 Results

From the $m = 8564$ recorded thermoelastic values, and, $h = 2 \times 1192 = 2384$ and $t = 2 \times (2731 + 250) = 5962$ boundary conditions on the internal and external boundaries, the Airy coefficients can be solved by forming a linear system of equation represented in matrix form as $[A]_{(m+h+t) \times k} \{c\}_{k \times 1} = \{d\}_{(m+h+t) \times 1}$. The number of equations, $m + h + t = 16,910$ will exceed the number of coefficients, k . The resulting overdetermined system of equations with which to evaluate the unknown

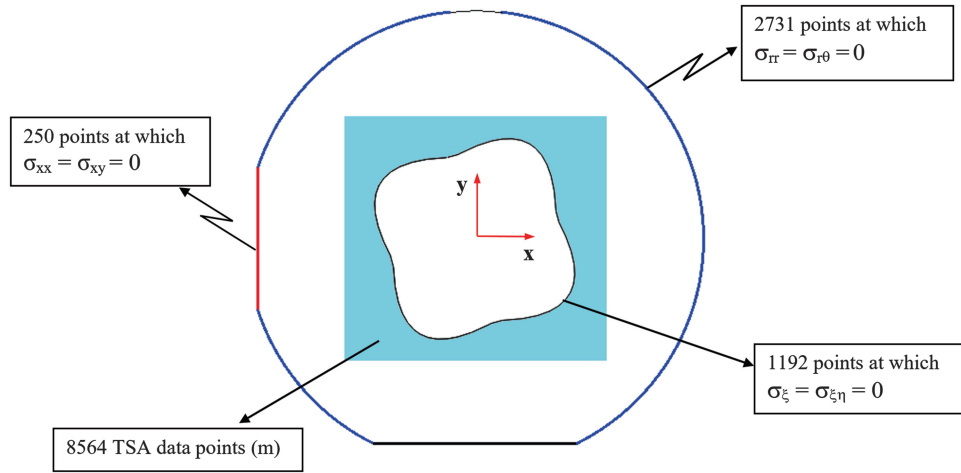


Fig. 2.2 Locations of TSA data and imposed traction-free boundary conditions

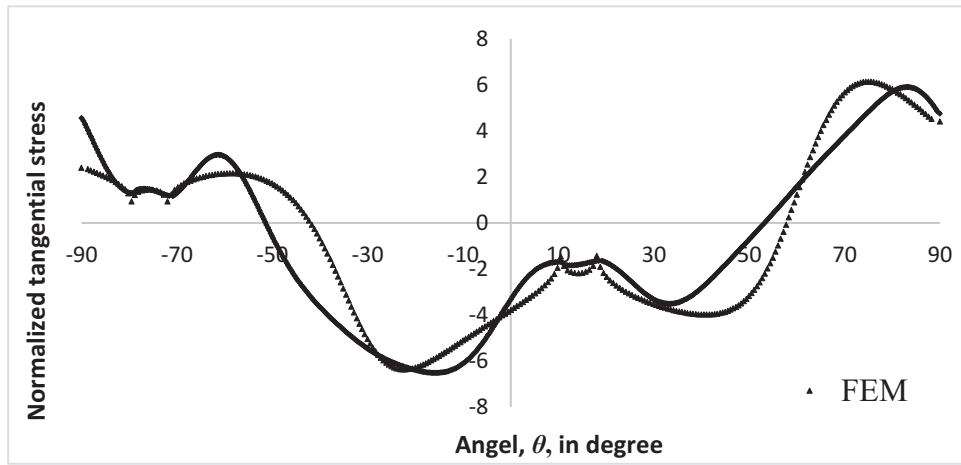


Fig. 2.3 Variations of tangential stress, $\sigma_{\eta\eta}$, on the edge of the irregularly-shaped hole from FEA and hybrid-TSA ($k = 103$ and $m + h + t = 16,910$)

Table 2.1 Strains $E_{\eta\eta}$ at locations on the internal boundary by each of hybrid-TSA, FEA (ANSYS), and strain gages for a static load of 1,334.46 N on structure of Fig. 2.1

Location on the inner surface of the hole	Strain value ($\mu\epsilon$)	Average strain value ($\mu\epsilon$)	Hybrid-TSA method	FEA (ANSYS)
$\theta = 58^\circ$	890	910	890	870
$\theta = 232^\circ$	930			
$\theta = 158^\circ$	-420	-410	-480	-440
$\theta = 338^\circ$	-400			

coefficients was solved using least-squares. The number of Airy coefficients to retain, $k = 103$, was assessed by monitoring the condition number of the respective Airy matrix, computing the Root Mean Square (RMS) for a series of different number of Airy coefficients and by comparing the reconstructed thermoelastic data with the actual measured thermoelastic signals.

With $\sigma_{\xi\xi}$ and $\sigma_{\xi\eta}$ in the $\xi\eta$ -coordinate system (tangential-normal) being numerically zero as dictated by imposing the traction-free conditions on the edge of the of the irregularly-shaped hole, the normalized tangential stress, $\sigma_{\eta\eta}/\sigma_0$, along the edge from FEA and hybrid-TSA is shown in Fig. 2.3. The results of this hybrid experiment based on discrete input values of S^* agree with ANSYS, including along edges where no input values were employed. The stresses are normalized with respect to a far-field stress $\sigma_0 = 1334.46/99 \times 9.53 = 1.415$ MPa.

Table 2.1 compares the strains from hybrid-TSA, FEA, and the strain gages. The good agreement between the current hybrid-TSA results and those from FEA and the strain gages provides strong confidence in the presently developed ability to obtain reliable stresses from recorded thermal information.

2.4 Summary, Discussion and Conclusions

A major contribution of this paper is the demonstrated ability to combine experimental (TSA), numerical (least-squares) and analytical (Airy stress) techniques for the full-field determination of the separate components of stresses at and in the neighborhood of the irregularly-shaped hole in a loaded finite arbitrarily-shaped structure, Fig. 2.1, and to do so without having to model the situation, know the external loading or constitutive properties, or differentiate the recorded data. This paper deals with an irregularly-shaped internal boundary and arbitrarily-shaped external boundary. The authors are unaware of prior utilization of Airy stress function to evaluate experimentally the stresses for such complex geometry of the plate in Fig. 2.1 using recorded load-induced thermal information.

References

1. Muskhelishvili, N.: Some basic problems of the mathematical theory of elasticity. Springer, Leyden (1977)
2. Lekhnitskii, S.G.: Anisotropic plates. Gordon & Breach Scientific Publishers, New York (1968)
3. Timoshenko, S., Goodier, J.: Theory of elasticity. McGraw-Hill Publishing Company, New York (1970)
4. Foust, B.E., Rowlands, R.E.: Thermoelastic determination of individual stresses in a diametrically loaded disk. *Strain*. **47**(2), 146–153 (2011)
5. Lin, S.-J., Matthys, D.R., Rowlands, R.E.: Separating stresses thermoelastically in a central circularly perforated plate using an airy stress function. *Strain*. **45**(6), 516–526 (2009)
6. Samad, W.A., Rowlands, R.E.: Full-field thermoelastic stress analysis of a finite structure containing an irregularly-shaped hole. *Exp. Mech.* **54**(3), 457–469 (2014)
7. Samad, W.A., Khaja, A.A., Kaliyanda, A.R., Rowlands, R.E.: Hybrid thermoelastic stress analysis of a pinned joint. *Exp. Mech.* **54**(4), 515–525 (2014)
8. Lin, S.-J., Quinn, S., Matthys, D.R., New, A.M., Kincaid, I.M., Boyce, B.R., Khaja, A.A., Rowlands, R.E.: Thermoelastic determination of individual stresses in vicinity of a near-edge hole beneath a concentrated load. *Exp. Mech.* **51**(6), 797–814 (2011)
9. Lin, S.J., Matthys, D.R., Samad, W.A., Khaja, A.A., Boyce, B.R., Rowlands, R.E.: Infrared stress analysis of unsymmetrically-loaded perforated member, ISEM-ACEM-SEM-7th ISEM'12, Taipei (2012)
10. Samad, W.A., Rowlands, R.E.: Hybrid thermoelastic analysis of an unsymmetrically-loaded structure containing an arbitrarily-shaped cutout. In: Residual stress, thermomechanics & infrared imaging, hybrid techniques and inverse problems, vol 8, pp. 51–57. Springer (2014)
11. Abdel Samad, W.: Hybrid full-field stress analysis of structures containing irregularly-shaped cutouts, PhD Thesis, University of Wisconsin-Madison (2013)
12. Lin, S.J., Matthys, D.R., Quinn, S., Davidson, J.P., Boyce, B.R., Khaja, A.A., Rowlands, R.E.: Stresses at and in the neighborhood of a near-edge hole in a plate subjected to an offset load from measured temperatures. *Eur. J. Mech. A Solids*. **39**, 209–217 (2013)
13. Kurunthottikkal Philip, S.: Stress analysis of a finite structure containing an asymmetrical, arbitrarily-shaped cutout based on recorded temperature data, Master Thesis, University of Wisconsin – Madison (2015)
14. Lin, S.T., Rowlands, R.E.: Thermoelastic stress analysis of orthotropic composites. *Exp. Mech.* **35**(3), 257–265 (1995)
15. Alshaya, A., Shuai, X., Rowlands, R.: Thermoelastic stress analysis of a finite orthotropic composite containing an elliptical hole. *Exp. Mech.* **56**(8), 1373–1384 (2016)
16. Alshaya, A.A.: Experimental, analytical and numerical analyses of orthotropic materials and biomechanics application, PhD Thesis, University of Wisconsin-Madison (2017)
17. Greene, R., Patterson, E., Rowlands, R.: Thermoelastic stress analysis. In: Sharpe, J., William, N. (eds.) Springer handbook of experimental solid mechanics, pp. 743–768. Springer, New York (2008)
18. Soutas-Little, R.W.: Elasticity. Dover Publications, Mineola (1999)

Residual Stress, Thermomechanics & Infrared Imaging,
Hybrid Techniques and Inverse Problems, Volume 8
Proceedings of the 2017 Annual Conference on
Experimental and Applied Mechanics
Baldi, A.; Considine, J.; Quinn, S.; Balandraud, X. (Eds.)
2018, VIII, 127 p. 108 illus., 93 illus. in color., Hardcover
ISBN: 978-3-319-62898-1